

Nanoscale

Accepted Manuscript



This is an *Accepted Manuscript*, which has been through the Royal Society of Chemistry peer review process and has been accepted for publication.

Accepted Manuscripts are published online shortly after acceptance, before technical editing, formatting and proof reading. Using this free service, authors can make their results available to the community, in citable form, before we publish the edited article. We will replace this *Accepted Manuscript* with the edited and formatted *Advance Article* as soon as it is available.

You can find more information about *Accepted Manuscripts* in the [Information for Authors](#).

Please note that technical editing may introduce minor changes to the text and/or graphics, which may alter content. The journal's standard [Terms & Conditions](#) and the [Ethical guidelines](#) still apply. In no event shall the Royal Society of Chemistry be held responsible for any errors or omissions in this *Accepted Manuscript* or any consequences arising from the use of any information it contains.

ARTICLE

Direct ultrasensitive electrical detection of prostate cancer biomarker with CMOS-compatible n- and p-type silicon nanowire sensor arrays

Cite this: DOI: 10.1039/x0xx00000x

Received 00th January 2012,
Accepted 00th January 2012

DOI: 10.1039/x0xx00000x

www.rsc.org/

Anran Gao^a, Na Lu^a, Pengfei Dai^a, Chunhai Fan^b, Yuelin Wang^{*a} and Tie Li^{*a}

Sensitive and quantitative analysis of proteins is central to disease diagnosis, drug screening, and proteomic studies. Here, a label-free, real-time, simultaneous and ultrasensitive prostate-specific antigen (PSA) sensor was developed using CMOS-compatible silicon nanowire field effect transistors (SiNW FET). Highly responsive n- and p-typed SiNW arrays were fabricated and integrated on a single chip with a complementary metal oxide semiconductor (CMOS) compatible anisotropic self-stop etching technique which eliminated the need for hybrid method. The incorporated n- and p-type nanowires revealed complementary electrical response upon PSA binding, providing a unique means of internal control for sensing signal verification. The highly selective, simultaneous and multiplexed detection of PSA marker at attomolar concentrations, a level useful for clinical diagnosis of prostate cancer, was demonstrated. The detection ability was corroborated to be effective by comparing the detection results at different pH values. Furthermore, the real-time measurement was also carried out in clinical relevant sample of blood serum, indicating the practicable development of rapid, robust, high-performance, and low-cost diagnostic systems.

Introduction

Many biomarkers have proven to have great potential to greatly improve disease diagnosis¹⁻⁴ and provide the basis for new therapeutic protocols⁵⁻⁷. For detecting small amounts of biomarkers in the early-stage of disease, it is of great importance to convert the biological information into an electronic signal⁸⁻¹⁰, especially for the diagnosis of complex disease like prostate cancer¹¹⁻¹³. Prostate specific antigen (PSA) has been proved to be an extremely useful marker for early detection of prostate cancer and in monitoring patients for disease progression and the effects of treatment^{14,15}. The development of techniques that allow rapid, multiplexed detection of many markers like PSA with high sensitivity and selectivity is very critical in health care. However, this goal has not been attained with any existing methods, including enzyme-linked immunosorbent assay (ELISA)¹⁶, surface plasmon resonance (SPR)^{17,18}, nanoparticles¹⁹⁻²², cantilever¹⁴, carbon nanotubes²³⁻²⁵, and so on. Silicon nanowire (SiNW) as biosensor has received considerable attention because of its high sensitive, rapid, label-free, and real-time detection capabilities^{8,26-29}. By exploiting these attractive properties, SiNWs have been designed for recognizing a wide range of targets³⁰⁻³⁷.

Recent biosensing literatures have reported the use of either n- or p-type nanowires as successful sensors for biological analytes sensing^{32,38-41}. Due to the fact that SiNWs-based biosensor is liable to the interference^{8,42}, possible electrical cross-talk and/or false-positive signals may occur²⁷, making detection with either n-type or p-type nanowire inadequate. Combining two types of nanowires for sensing may offer an interesting comparison and also provide novel sensing strategies. Notably, the incorporation of both n- and p-type

nanowires in a single sensor chip enables discrimination against false positives by correlating the response versus time from the two types of device elements²⁷. Therefore, the device ability of multiplexed detection is believed to be especially important in disease diagnosis. However, the combination of different types of nanowires for multiplexed detection has not, however, been reported too much. Zheng et al.²⁷ have given a pioneering and creative study addressing highly selective and sensitive multiplexed detection of cancer markers using silicon nanowire field effect device. However, their SiNW devices are fabricated based on a “bottom-up” approach and rely on the assembly of grown SiNWs, which nevertheless inherently suffers from the limitations of complex integration, making large scale production impossible^{26,43-47}. Therefore, in order to simplify the fabrication process, lower the cost, and thus result in a more robust and portable device, the development of new manufacturing approach is necessary.

In this paper, we have developed a “top-down” method which has mass manufacturing ability and potential compatibility with silicon industry. The n- and p-type nanowire arrays are integrated on a single sensor chip by ion doping based on optical lithography and anisotropic wet etching with tetramethylammonium hydroxide (TMAH). The configuration allows multiplexed detection, enables discrimination of possible electrical cross-talk and/or false-positive signals by correlating the response versus time from the two types of device, facilitated object analysis and thus resulted in a more robust protocol. We demonstrated highly selective, simultaneous and multiplexed detection of PSA marker at attomolar concentrations using SiNW field-effect devices. In

addition, the real-time measurement was also carried out in clinical relevant sample of blood serum, indicating the practicable development of rapid, robust, high-performance, and low-cost diagnostic systems.

Experimental section

Chemicals and materials

The 3-aminopropyltriethoxysilane (APTES), 1-ethyl-3-(3-dimethylaminopropyl) carbodiimide (EDC), N-hydroxysuccinimide (NHS), bovine serum albumin (BSA), human serum, glutaraldehyde and ethanolamine were purchased from Sigma-Aldrich (U.S.A.) and used as received. Other chemicals were obtained from Sinopharm Chemical Reagent Co., Ltd. (Shanghai, China). Solutions were prepared with Milli-Q deionized water (18 M Ω cm, Millipore) from a Millipore system. PSA were purchased from Fitzgerald (Acton, MA, USA). Monoclonal antibody for PSA was purchased from US Biological Inc (Swampscott, MA, USA). The proteins were used without further purification and diluted to the desired concentrations with the assay buffer.

Fabrication of SiNW arrays

Nanowire FET devices were fabricated from silicon-on-insulator (SOI) wafers as described previously³⁵. Briefly, commercially available (100) oriented SIMOX silicon-on-insulator (SOI) wafers with light boron adulteration of $5 \times 10^{15} \text{cm}^{-3}$ were used in this method. The top silicon layer of the wafer was thinned to 70–80 nm with a 100 nm thermally oxidized SiO₂ layer upon it by repetitions of oxidation and buffered HF etching. Optical lithography and buffered HF etching were then applied to pattern the SiO₂ mask. Ion implantation of boron adulterant with doping dose $6 \times 10^{15} \text{cm}^{-3}$ energy 70 Kev and phosphor adulterant with doping dose $5 \times 10^{15} \text{cm}^{-3}$ energy 40 Kev, followed by 30 min of annealing in nitrogen at 1100 °C, was separately carried out to form an effective contact region for p- and n-type device with a concentration of 10^{20}cm^{-3} . The NW-FET device regions were first defined with a wet chemical etch (tetramethylammonium hydroxide, TMAH), which etches Si(111) planes at $\sim 1/100$ the rate of all other planes. Then a thin nitride film (50 nm) was deposited by low-pressure-chemical-vapor-deposition (LPCVD) to protect the (111) plane previously defined. After the nitride film was patterned by ion-beam etching, the 100 nm SiO₂ layer beneath was totally removed by diluted HF. Then by using TMAH for the second time, we finally got controllable SiNW arrays with a triangular cross section after removing the nitride film. It should be noted that this etch produces triangular devices due to the (100) orientation of the SOI wafers. To decrease the density of surface dangling bonds on the Si surface and increase the stability of the sensors, a high-quality SiO₂ layer was finally thermally oxidized on the silicon nanowire surfaces.

Surface modification

The SiNW array was first cleaned in a piranha solution at 90 °C in order to clean the sample surfaces as well as to generate more hydrophilic surfaces hydroxyl terminating the silicon-oxide surface. Then it was functionalized by exposing the surface to APTES solution (2% ethanol) overnight, followed by rinsing with absolute ethanol to remove unreacted

APTES. After that, a self-assembled monolayer with terminal amino group was prepared by blowing the surface with nitrogen, followed by heating at 120 °C for 5 min. A biofunctional linker, glutaraldehyde, was then covalently attached onto the amine-terminated surface by immersing the chip in a solution of 10% glutaraldehyde in buffer solution (20 mM NaCl, 10 mM phosphate, pH 7.4) at 37 °C for 1 h. Antibody attachment on the SiNW surface was carried out by exposing SiNWs to 50 $\mu\text{g}/\text{ml}$ antibody of PSA (anti-PSA) in buffer solution at 37 °C for 2 h, followed by thoroughly washing with the same buffer. In order to prevent nonspecific binding of proteins in the detection step, the unreacted aldehydic groups on SiNW surface were passivated by applying 100 mM ethanolamine solution in buffer solution at 37 °C for 1 h, followed by washing with the same buffer.

Sensing Apparatus and Parameters

For PSA sensing, the measurements were performed by using a Keithley 4200 semiconductor parameter analyzer (Keithley Instruments Inc., Cleveland, OH). For sensing measurements, we used $V_{\text{DS}} = 1\text{V}$, $V_{\text{GS}} = 7\text{V}$ for n-type SiNWs and $V_{\text{DS}} = -1\text{V}$, $V_{\text{GS}} = -11\text{V}$ for p-type SiNWs, respectively. All solutions used in hybridization studies were 0.01 \times PBS, in which Debye length is sufficiently long to ensure effective sensing during the capture process. The current through the SiNW device was monitored while immersed in buffer solution proceeded to establish the baseline current, relative to which changes in current would be measured. Each measurement was carried out on a distinct device.

Serum Assays

Sera were taken from healthy donors. In serum assays, PSA was spiked to 100% human serum and diluted to different concentrations. Measurements were carried out using the same protocol as in the buffer solution.

Results and discussion

The sensitivity of SiNW FET capable of sensing the presence of even a small amount of bound charged species is critically depend upon its size and surface to volume ratio. In this work, silicon nanowires with controllable size and reproducibility were fabricated with a novel CMOS compatible anisotropic wet etching approach. Conventional optical lithography was combined with anisotropic wet etching by tetramethylammonium hydroxide (TMAH), which etches Si (111) planes 100 times slower than other planes⁴⁸, instead of using expensive electron beam lithography. Since the dry oxidization of silicon down nanometer level is a self-limiting process^{49, 50} and the lateral etching rate is very slow, the width of SiNWs could be precisely controlled by controlling the etching time and using self-limiting oxidization. In addition, this approach allows retention of pattern definition and smooth edge imperfections not aligned to the (111) plane, an effect that overcomes the limitations of traditional manufacturing methods⁴⁸.

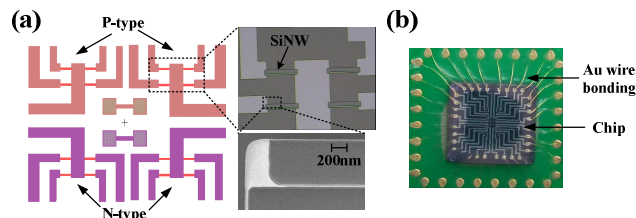


Figure 1 (a) Schematic showing the layout of the SiNW device arrays on the chip, the optical micrograph of a quarter of completed SiNW array and zoomed-in scanning electron microscopy image of a nanowire. A total of 4 clusters of 4 nanowires each are available for use, potentially allowing for simultaneous, multiplexed detection of assorted proteins. (b) Photograph of a completed SiNW-FET device. In the chip, aluminum was used as contact metal, and gold were used as leading wires.

The completed SiNW sensor chip consists of 4 clusters including electrically addressable and well-ordered arrays, contact lines and pads. A schematic array layout and fabricated silicon nanowires are provided in Figure 1a. As illustrated in Figure 1a, the SiNWs are grouped in cluster and each cluster is composed of 4 individually addressable nanowires. The layout including both p- and n-type nanowires is suitable for multiplexed detection as each cluster may serve as one sensing unit for a particular molecule. The optical micrograph of a quarter of completed SiNW array shows that nanowires are uniform and well-ordered for both p- and n-type devices. The zoom-in scanning electron microscopy image of a representative SiNW was observed to be well-shaped, highly uniform, and well-aligned with width of about 70 nm. Owing to the planarization and slow Si (111) rate of etch, the nanowire is with high quality. The dimension of the SiNWs can be controlled to different sizes, ranging from 20–200 nm, while its length may vary from a few to 100 μm with precise control. The small diameter of the NWs ensures high sensitivity while the long length enables multi-copy detection. The size and conductance distributions of the fabricated SiNWs (Supporting Information Figure S1) indicate the fabricated SiNWs were uniform and well-distributed in conductance.

The photography of a completed SiNW device wire bonded onto a printed circuit board was illustrated in Figure 1b. In order to gain relative stable contact properties, we used aluminum as contact metal, aurum as bonding wires and silicon rubber as protective layer for experiments in aqueous environment. Significantly, only the silicon nanowires were exposed to air/solution while other parts were coated with silicon nitride on the chip, guaranteeing the high sensitivity of the nanosensor⁵¹.

The quality of manufactured SiNWs was verified by electrical characterization of both p- and n-type nanowire FET devices (Figure S2, Supporting Information). Both n- and p-type devices yield typical gate modulation of field-effect devices, demonstrating excellent transfer characteristic. Electrical characterization verifies that this fabrication approach is capable of producing devices with high controllability and high quality.

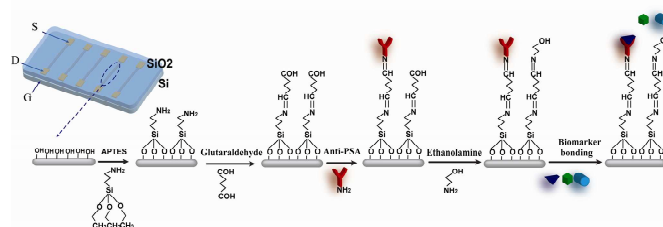


Figure 2 Schematic illustration of chemical process for real-time and label-free electrical detection of PSA.

In this study, silicon nanowire biosensors for detection of PSA biomarker were realized by immobilizing specific antibodies onto SiNW surface. The details are illustrated in Figure 2. The SiNW surface with oxide coating on it was firstly modified with conventional silane chemistry, APTES, as described in experimental section, generating monolayer with terminal amine group. The glutaraldehyde was then modified on SiNW surface, followed by covalently attachment of anti-PSA monoclonal antibody, a specific ligand for PSA protein. Finally, after the passivation process of SiNW surface with ethanolamine, the freshly prepared antibody-functionalized SiNW chips proceeded immediately to electrical testing.

In this paper, mixing cells (or called solution chamber) are used for solutions deliver. This cell, a cone-shaped, plastic sample holder, is placed over the nanosensor chip and allows the solution to be delivered from the top aperture. In this setup, different solutions are delivered by replacement methods and the analyte diffuses isotropically until it reaches the sensor surface. In addition, injection of the solution tangential to the NW-FET sensor significantly decreased the detection response times compared to those observed in NW-FETs that used microfluidic channels for the detection of similar target molecules^{52,53}.

The change of SiNW characteristics after different treatments was studied and thus further elucidated the field-effect of the SiNWs. Upon exposure to different buffer solutions, the output I_{DS}/V_{DS} characteristic curves of n- and p-type device were both modified (Figure 3a, 3b). A buffer solution of $0.01\times$ PBS (pH 7.4) was used for PSA detection experiments so as to minimize this counter ion screening effect (Figure S3, Supporting Information). The change with different solutions that form a different electrostatic charge environment of SiNW is crucial in explaining the behavior of the SiNW biomolecular sensor. Consequently, the electrostatic charges associated with the biomolecular reactions play the role of an effective gate voltage and the detection process does not introduce significant changes in the electronic structure of the nanowire.

Significantly, the $I_{DS}-V_{DS}$ curves of n- and p-type SiNW device change in opposite directions after the modification of anti-PSA and specific PSA bonding. In the case of n-type silicon nanowire device, applying a positive gate voltage accumulates carriers and increases the current, whereas applying a negative gate voltage leads to a depletion of carriers and a reduction of current (the opposite effect occurs in p-type SiNW device). The net charge of anti-PSA with isoelectric point (Pi) ~ 8 used in the study is positive, while PSA is negatively charged, which is expected from isoelectric point (Pi) of PSA, 6.8⁵⁴, and pH, 7.4, of our experiments. Thus, one would expect an increase in current on anti-PSA binding and the bonding of PSA to the antibody receptor on a n-type SiNW

results in the depletion of carriers and a decrease of SiNW current, whereas the opposite response was observed for a p-type SiNW device.

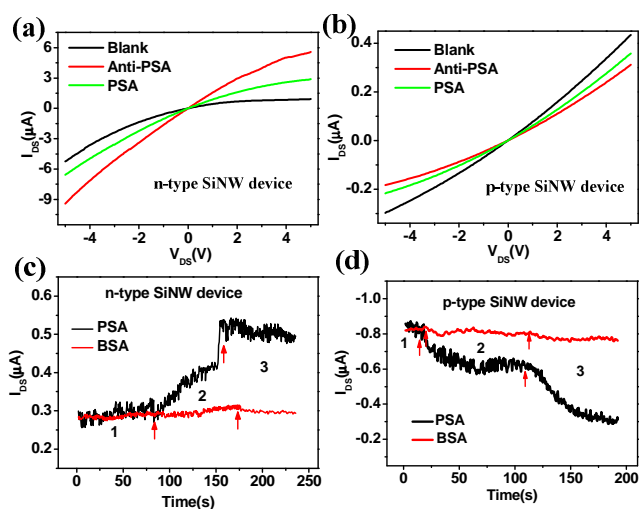


Figure 3 (a) (b) The I - V characteristics of the (a) n- and (b) p-type SiNW when exposed to different solutions in the process of PSA detection. The I_{DS}/V_{DS} curves of the SiNW with back-gate bias at various stages during the surface functionalization procedure was obtained by sweeping the applied drain-source voltage from -5 V to 5 V, while the V_{GS} is 7 V for n-type device and -11 V for p-type device. (c) (d) Plots of current versus time for (c) n- and (d) p-type of SiNW-FETs at pH 6.0. Region 1 corresponds to buffer solution, region 2 corresponds to the addition of 10 fg/ml PSA and region 3 corresponds to the addition of 1 pg/ml PSA. The arrows mark the points when the solutions were introduced. The length of SiNWs used in this study was of 16 μm

As an initial study of multiplexed detection, Silicon nanowire arrays containing both n-type and p-type devices modified with anti-PSA were used for real-time and electrical PSA detection. Notably, the current versus time data recorded from n-type nanowire (Figure 3c) and p-type nanowire (Figure 3d) after introduction of 10 fg/ml and 1 pg/ml PSA showed complementary response. PSA was positively charged at pH 6.0, accumulating carriers of n-type nanowire and thus increasing the current, whereas the positively charged PSA reduced current of p-type device. The n- and p-type devices showed current increase and decrease, respectively, and the magnitude of the current change in the two devices was comparative. The relative current change of both types of device is almost same, ~30% for 10 fM PSA and ~50% for 1 pM PSA. The comparison indicates that the n- and p-type nanowires can sense the target at almost the same sensitivity, and both types of nanowires are highly responsive. The multiplexed electrical detection with nanowire devices revealing complementary signals from n- and p-type devices provides a simple yet robust means for detection false-positive signals from either electrical noise or nonspecific binding of protein onto nanowire device. By correlating the change of current signals in both devices, which occurs at points when buffer solutions are changed, the multiplexing capability of our device can distinguish unambiguously noise from specific protein binding signals, especially for ultralow concentrations of the target. Therefore,

the incorporation of both n- and p-type nanowires in a single sensor chip will facilitate object analysis, reduce the number of false positive and false negative incidents, and result in a more robust and portable protocol in general.

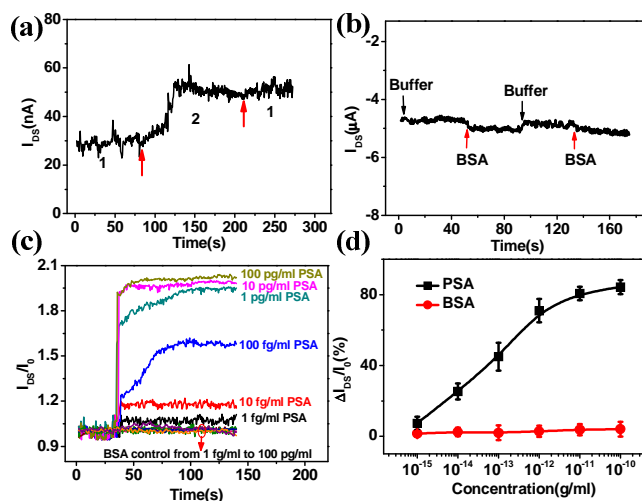


Figure 4 (a) Plot of current versus time for anti-PSA modified n-type SiNW-FET, where region 1 stands for the presence of buffer solution and region 2 for the addition of 1 pg/ml PSA. The arrows mark the points when the solutions were changed. (b) Plot of current versus time of p-type SiNW device for real-time detection of 10 mg/ml BSA. (c) Plots of normalized current change versus time with PSA at a series of concentrations (1 fg/ml, 10 fg/ml, 100 fg/ml, 1 pg/ml, 10 pg/ml and 100 pg/ml) for anti-PSA modified n-type SiNW-FET. Hybridization was demonstrated in 0.01× PBS. (d) Normalized current change as a function of the logarithm of PSA concentration. The length of all SiNWs used in the experiments was 6 μm

A second test of multiplexing capability using a device array consisting of several silicon nanowires was carried out at pH 6.0 by real time monitoring the current change. Here, a relative change of the current is defined for the response of the device to the PSA: $\Delta I/I_0$, where ΔI is the change of the current in the assay, and I_0 represents the value of the initial current ($t = 0$). As illustrate in Figure 4a, for one nanowire in the array, when the buffer solution (0.01×) flowed through the anti-PSA modified SiNW sensor surface, the electrical response of the SiNW-FET remained stable. Significantly, when the solution containing 1 pg/ml PSA was introduced, the time-dependent current measurement exhibited a rapid current increase. Notably, the current remained nearly unchanged after washing with buffer solution without PSA, indicating the electrical current change is caused by the specific binding events and there is little nonspecific bonding. The peak is caused by continually pumping with pipette during surface washing.

As a control experiment to further quantify any background effect due to the nonspecific binding of noncognate proteins to the SiNW device surface, a SiNW device in the array was functionalized with anti-PSA capture antibodies was tested (Figure 4b). Upon the addition of 10 mg/ml bovine serum

albumin solution (BSA, pI 4.7)⁵⁵ in 0.01× PBS, the SiNW device demonstrated ~4% relative current change, which is negligible compare with ~70% relative current change induced by 1 pg/ml PSA in Figure 4a. This suggests that the nonspecific binding and adsorption of BSA protein molecules, even at a 10⁹-fold higher concentration than used in Figure 4a, may effectively be omitted from consideration.

The sensitivity of the SiNW-FET sensor was interrogated by challenging it with a series of concentrations of PSA. Solutions of PSA of various concentrations were prepared by dissolving and serially diluting pure PSA in 0.01×PBS. SiNWs were functionalized with anti-PSA antibodies and used in experiments for detection in these analyte solutions. The real-time response of current upon injection of various concentrations of PSA was illustrated in Figure 4c. Specifically, Known concentrations of PSA were added after a stable reading with 0.01× PBS buffer was achieved. The introduction of 1fg/ml, 10fg/ml, 100fg/ml, 1pg/ml, 10pg/ml and 100pg/ml solutions of PSA resulted in current change of ~7%, ~25%, ~41%, ~76%, ~80% and ~84%, respectively. Compared with Figure 4a, the relative current change for 1 pg/ml PSA is both about ~70%, demonstrating excellent reproducibility of the devices. The little nonspecific binding and adsorption of other molecules was also demonstrated with a series of concentrations of BSA. The SiNW response as a function of PSA and BSA concentration is shown in Figure 4d. The electrical current change increased monotonously with the logarithm of PSA concentration, whereas the current remained nearly unchanged with the logarithm of BSA concentration. The error bars in Figure 4d represent device-to-device standard deviations for measurements obtained from three nanowires. The direct, label-free detection of PSA down to 1fg/ml or ~30aM demonstrates the ultrahigh sensitivity of our nanosensor. The detection limit will increase capacity of clinical diagnosis because of the ultralow concentrations of specific markers in clinical samples.

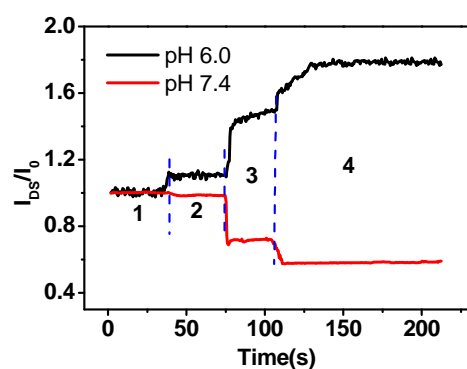


Figure 5 Plot of current versus time for anti-PSA modified n-type SiNW-FET at pH 6.0 and 7.4, where region 1 stands for the presence of buffer solution, region 2 for the addition of 10 fg/ml PSA, region 3 for the addition of 100 fg/ml PSA and region 4 for the addition of 1 pg/ml PSA. The arrows mark the points when the solutions were changed. The length of SiNWs used was of 40 μm

To further verify that the current change of SiNW-FET sensors was caused by the specific binding of PSA, PSA solution at pH 6.0 and pH 7.4 was separately injected onto the SiNW sensor arrays and the SiNW current was real-time monitored. Due to the pI 6.8 of PSA⁵², the net charge of PSA is positive at pH 6.0 and negative at pH 7.4. Therefore, one would expect an increase/decrease in current at pH 6.0/7.4 on PSA binding to the n-type SiNW-FET sensor. As illustrated in Figure 5, the current versus time data for the detection of PSA shows opposite change in current at pH 6.0 and pH 7.4, which provides the evidence of the reliable detection of PSA. As the PSA solutions of 10fg/ml, 100fg/ml, and 1pg/ml were sequentially introduced onto SiNW array, the current of SiNW devices showed concentration dependent increases and decreases at pH 6.0 and pH 7.4, respectively. Significantly, the magnitude of the current change at pH 6.0 is slightly larger than that at pH 7.4. This result is due to the different quantity of charges of PSA at different pH, as expected from the pI of PSA 6.8, and the pH values. This method also enables our SiNW-FET sensor to be applied for exploring pI values of biomolecules and measuring pH values of solution in low-volume⁵⁶.

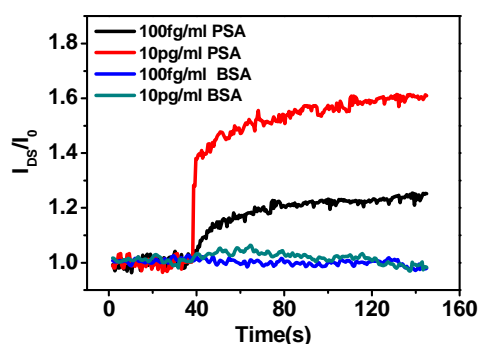


Figure 6 Current versus time data recorded for the detection of PSA and BSA in human serum on n-type SiNW arrays with length of 16 μm and functionalized with anti-PSA.

For medical point-of-care applications, it is of special importance to accurately detect low concentrations of biomarkers in clinically relevant samples, such as human blood serum. Hence, we investigated detection of PSA in human blood serum environment (Figure 6). The measurement was carried out using anti-PSA functionalized n-type SiNW arrays. The raw serum was desalted using and diluted to the original protein concentration with 0.01× PBS. An initial baseline for the current of the SiNW device was established by injecting desalted serum solution not containing PSA onto nanowire. Upon subsequent addition of the PSA-containing serum solution, the current of the device immediately increased and eventually stabilized. The concentration dependent current change of SiNW device in serum samples clearly demonstrates its capability of detection of cancer marker in real-sample assay with high sensitivity. As a control experiment, the introduction of BSA of the same concentrations induced negligible current change, demonstrating little nonspecific bonding on SiNW sensor.

Conclusions

Here, we present label-free, real-time, multiplexed and complementary detection of prostate specific antigen (PSA) with high selectivity and attomolar sensitivity using n- and p-type antibody-functionalized silicon nanowire field-effect sensors. The n- and p-type nanowires are combined together for the detection of PSA, which revealed complementary electrical response upon PSA binding. The detection ability was characterized in both ideal and clinically relevant samples of blood serum. Furthermore, by comparing the detection results at different pH values the detection of PSA in solution has been demonstrated to be effective as low as 1fg/ml, a level useful for clinical diagnosis of prostate cancer. Given the extraordinary ability for label-free and ultrasensitive biomolecule detection, mass reproducible ability, CMOS compatibility, as well as low cost character, the SiNW device was expected to provide the basis for new therapeutic protocols.

Acknowledgements

We appreciate financial support from National Basic Research Program of China (973 Program No. 2012CB933301), Fund for Creative Research of National Natural Science Foundation of China (No. 61321492), Key project of National Natural Science Foundation of China (No. 91323304, No. 91123037, No. 81201358), FP-7 PEOPLE-2010-IRSES project ECNANOMAN (No. 269219) Shanghai International Science and Technology Cooperation Foundation project (No. 12410707300), Shanghai Youth Science and technology talent sailing project (No. 14YF1407200).

Notes and references

^a State Key Laboratories of Transducer Technology & Science and Technology on Micro-system Laboratory, Shanghai Institute of Microsystem and Information Technology, Chinese Academy of Sciences, 200050, Shanghai, China.

^b Division of Physical Biology and Bioimaging Center, Shanghai Synchrotron Radiation Facility, Shanghai Institute of Applied Physics, Chinese Academy of Sciences, 201800, Shanghai, China.

Electronic Supplementary Information (ESI) available: Electrical characterization of fabricated n- and p-type nanowires, influence of Debye Screening on PSA sensing. See DOI: 10.1039/b000000x/

- R. Etzioni, N. Urban, S. Ramsey, M. McIntosh, S. Schwartz, B. Reid, J. Radich, G. Anderson and L. Hartwell, *Nature Reviews Cancer*, 2003, 3, 243-252.
- C. Sander, *Science*, 2000, 287, 1977-1978.
- P. R. Srinivas, B. S. Kramer and S. Srivastava, *Lancet Oncology*, 2001, 2, 698-704.
- G.-J. Zhang and Y. Ning, *Analytica Chimica Acta*, 749, 1-15.
- S. Boccaletti, V. Latora, Y. Moreno, M. Chavez and D. U. Hwang, *Physics Reports-Review Section of Physics Letters*, 2006, 424, 175-308.
- J. A. Ludwig and J. N. Weinstein, *Nature Reviews Cancer*, 2005, 5, 845-856.
- T. S. Pui, A. Agarwal, F. Ye, Z. Q. Ton, Y. X. Huang and P. Chen, *Nanoscale*, 2009, 1, 159-163.
- A. R. Gao, N. L. Zou, P. F. Dai, N. Lu, T. Li, Y. L. Wang, J. L. Zhao and H. J. Mao, *Nano Letters*, 2013, 13, 4123-4130.
- F. Patolsky and C. M. Lieber, *Materials today*, 2005, 8, 20-28.
- A. R. Gao, N. Lu, Y. C. Wang, P. F. Dai, T. Li, X. L. Gao, Y. L. Wang and C. H. Fan, *Nano Letters*, 2012, 12, 5262-5268.
- J. J. Hornberg, F. J. Bruggeman, H. V. Westerhoff and J. Lankelma, *Biosystems*, 2006, 83, 81-90.
- C. Li, M. Curreli, H. Lin, B. Lei, F. Ishikawa, R. Datar, R. J. Cote, M. E. Thompson and C. Zhou, *Journal of the American Chemical Society*, 2005, 127, 12484-12485.
- K. W. Wee, G. Y. Kang, J. Park, J. Y. Kang, D. S. Yoon, J. H. Park and T. S. Kim, *Biosensors and Bioelectronics*, 2005, 20, 1932-1938.
- G. H. Wu, R. H. Datar, K. M. Hansen, T. Thundat, R. J. Cote and A. Majumdar, *Nature Biotechnology*, 2001, 19, 856-860.
- H. Xie, S. C. Luo and H. H. Yu, *Small*, 2009, 5, 2611-2617.
- A. M. Ward, J. W. F. Catto and F. C. Hamdy, *Annals of Clinical Biochemistry*, 2001, 38, 633-651.
- S. F. Chou, W. L. Hsu, J. M. Hwang and C. Y. Chen, *Biosensors & Bioelectronics*, 2004, 19, 999-1005.
- C. Campagnolo, K. J. Meyers, T. Ryan, R. C. Atkinson, Y. T. Chen, M. J. Scanlan, G. Ritter, L. J. Old and C. A. Batt, *Journal of Biochemical and Biophysical Methods*, 2004, 61, 283-298.
- J. M. Nam, C. S. Thaxton and C. A. Mirkin, *Science*, 2003, 301, 1884-1886.
- T. Soukka, J. Paukkunen, H. Harma, S. Lonnberg, H. Lindroos and T. Lovgren, *Clinical Chemistry*, 2001, 47, 1269-1278.
- X. H. Gao, Y. Y. Cui, R. M. Levenson, L. W. K. Chung and S. M. Nie, *Nature Biotechnology*, 2004, 22, 969-976.
- P. Alivisatos, *Nature Biotechnology*, 2004, 22, 47-52.
- J. J. Gooding, R. Wibowo, J. Q. Liu, W. R. Yang, D. Losic, S. Orbons, F. J. Mearns, J. G. Shapter and D. B. Hibbert, *Journal of the American Chemical Society*, 2003, 125, 9006-9007.
- J. B. Chang, S. Mao, Y. Zhang, S. M. Cui, D. A. Steeber and J. H. Chen, *Biosensors & Bioelectronics*, 2013, 42, 186-192.
- R. J. Chen, S. Bangsaruntip, K. A. Drouvalakis, N. W. S. Kam, M. Shim, Y. M. Li, W. Kim, P. J. Utz and H. J. Dai, *Proceedings of the National Academy of Sciences of the United States of America*, 2003, 100, 4984-4989.
- E. Stern, J. F. Klemic, D. A. Routenberg, P. N. Wyrembak, D. B. Turner-Evans, A. D. Hamilton, D. A. LaVan, T. M. Fahmy and M. A. Reed, *Nature*, 2007, 445, 519-522.
- G. F. Zheng, F. Patolsky, Y. Cui, W. U. Wang and C. M. Lieber, *Nature Biotechnology*, 2005, 23, 1294-1301.
- S. Su, Y. He, S. P. Song, D. Li, L. H. Wang, C. H. Fan and S. T. Lee, *Nanoscale*, 2010, 2, 1704-1707.
- T.-S. Pui, A. Agarwal, F. Ye, Z.-Q. Tou, Y. Huang and P. Chen, *Nanoscale*, 2009, 1, 159-163.
- F. Patolsky, G. F. Zheng, O. Hayden, M. Lakadamyali, X. W. Zhuang and C. M. Lieber, *Proceedings of the National Academy of Sciences of the United States of America*, 2004, 101, 14017-14022.
- F. Patolsky, G. F. Zheng and C. M. Lieber, *Nature Protocols*, 2006, 1, 1711-1724.
- F. Patolsky, G. F. Zheng and C. M. Lieber, *Analytical Chemistry*, 2006, 78, 4260-4269.
- F. Patolsky, G. Zheng and C. M. Lieber, *Nanomedicine*, 2006, 1, 51-65.
- A. R. Gao, P. F. Dai, N. Lu, T. Li and Y. L. Wang, 2012 International Conference on Manipulation, Manufacturing and Measurement on the Nanoscale (3m-Nano), 2012, 113-116.
- A. R. Gao, N. Lu, P. F. Dai, T. Li, H. Pei, X. L. Gao, Y. B. Gong, Y. L. Wang and C. H. Fan, *Nano Letters*, 2011, 11, 3974-3978.

36. E. N. Dattoli, A. V. Davydov and K. D. Benkstein, *Nanoscale*, 2012, 4, 1760-1769.
37. G.-J. Zhang, L. Zhang, M. J. Huang, Z. H. H. Luo, G. K. I. Tay, E.-J. A. Lim, T. G. Kang and Y. Chen, *Sensors and Actuators B: Chemical*, 146, 138-144.
38. G.-J. Zhang, G. Zhang, J. H. Chua, R.-E. Chee, E. H. Wong, A. Agarwal, K. D. Buddharaju, N. Singh, Z. Gao and N. Balasubramanian, *Nano Letters*, 2008, 8, 1066-1070.
39. Z. Gao, A. Agarwal, A. D. Trigg, N. Singh, C. Fang, C.-H. Tung, Y. Fan, K. D. Buddharaju and J. Kong, *Analytical Chemistry*, 2007, 79, 3291-3297.
40. A. Agarwal, K. Buddharaju, I. Lao, N. Singh, N. Balasubramanian and D. Kwong, *Sensors and Actuators A: Physical*, 2008, 145, 207-213.
41. T.-S. Pui, A. Agarwal, F. Ye, Y. Huang and P. Chen, *Biosensors and Bioelectronics*, 26, 2746-2750.
42. Y. Im, C. Lee, R. P. Vasquez, M. A. Bangar, N. V. Myung, E. J. Menke, R. M. Penner and M. H. Yun, *Small*, 2006, 2, 356-358.
43. I. Park, Z. Li, A. P. Pisano and R. S. Williams, *Nanotechnology*, 21, 015501.
44. W. Lu and C. M. Lieber, *Nature Materials*, 2007, 6, 841-850.
45. E. Stern, A. Vacic and M. A. Reed, *Electron Devices, IEEE Transactions on*, 2008, 55, 3119-3130.
46. E. Stern, A. Vacic, N. K. Rajan, J. M. Criscione, J. Park, B. R. Ilic, D. J. Mooney, M. A. Reed and T. M. Fahmy, *Nature nanotechnology*, 5, 138-142.
47. K. N. Lee, S. W. Jung, K. S. Shin, W. H. Kim, M. H. Lee and W. K. Seong, *Small*, 2008, 4, 642-648.
48. O. Tabata, R. Asahi, H. Funabashi, K. Shimaoka and S. Sugiyama, *Sensors and Actuators a-Physical*, 1992, 34, 51-57.
49. M. Grydlik, M. Brehm, F. Hackl, H. Groiss, T. Fromherz, F. Schaffler and G. Bauer, *New Journal of Physics*, 2010, 12.
50. P. Sievila, N. Chekurov and I. Tittonen, *Nanotechnology*, 2010, 21.
51. E. Stern, R. Wagner, F. J. Sigworth, R. Breaker, T. M. Fahmy and M. A. Reed, *Nano Letters*, 2007, 7, 3405-3409.
52. Y. L. Bunimovich, Y. S. Shin, W.-S. Yeo, M. Amori, G. Kwong and J. R. Heath, *J. Am. Chem. Soc.*, 2006, 128(50), 16323-16331.
53. J. Hahn and C. M. Lieber, *Nano Letters*, 2004, 4, 51-54.
54. D. A. Armbruster, *Clinical Chemistry*, 1993, 39, 181-195.
55. Z. G. Peng, K. Hidajat and M. S. Uddin, *Journal of Colloid and Interface Science*, 2004, 271, 277-283.
56. A. Kim, C. S. Ah, H. Y. Yu, J. H. Yang, I. B. Baek, C. G. Ahn, C. W. Park, M. S. Jun and S. Lee, *Applied Physics Letters*, 2007, 91.